Energy, Environment and Storage

Journal Homepage: www.enenstrg.com

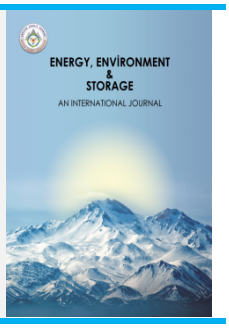

Numerical Analysis of The Multilayer Structures Melting with Different Hole Network with Phase Change Material

Elanur Baki Sezgin[1], Mustafa Yasin Gökaslan [2*], İrfan Uçkan [3]

[1]*Department of Mechanical Engineering, Institute of Natural and Applied Sciences,Yüzüncü Yıl University,Van,Turkey 0000-0001-7982-371X*

[2]*Department of Mechanical Engineering, Faculty of Engineering, Yüzüncü Yıl University, Van, Turkey 0000-0003-3859-8485*

[3]*Department of Mechanical Engineering, Faculty of Engineering, Yüzüncü Yıl University, Van, Turkey 0000-0003-3679-5661*

ABSTRACT. Phase change materials (PCM) are used with different geometries increase thermal performance. The thermal performance of the geometries on phase change materials have been investigated. For thermal energy storage systems (TES), porous structures are widely used to increase the thermal performance of the PCM. In addition, geometric parameters affect heat transfer, flow and melting solidification. In this work, the thermal performance of multilayer structure with different surface geometries and the control of the melt fraction of the PCM was investigated in terms of energy efficiency. The results were obtained by modeling the studies in the Computational Fluid Dynamics (CFD) program. The physical model was obtained by creating a multi-layer porous structure with different surface geometries in each layer, thanks to the additive system. Modeling was carried out for natural convection depending on time. Paraffin was used as the PCM. The melting temperature of the paraffin used is 41 °C and the latent heat of fusion is 165 kJ/kg. In the present work, the distribution of melting isotherms gives more homogeneous results for the selected geometry. The results of PCM multilayer structure and other geometries were compared under the same conditions and it was seen that the multilayer structure improved the thermal performance. All melting graphs range from 0-1 (0: solid, 1: liquid). The results obtained for the selected geometry show that the melting value is between 0.8-0.9. In addition, the proposed physical model is a subject that can be encountered in engineering applications, thermal design engineering. In this respect, it is thought that the results obtained from the study, especially in the field of energy storage, will fill an important gap.

Keywords: Energy storage, Phase change material, Numerical analysis, Multi-layer structure.

Article History: Received 18.07.2023; Accepted: 29.08.2023; Available online:30.09.2023
Doi : https://doi.org/10.52924/ZBHA5406

1. INTRODUCTION

Energy storage has gained a lot of importance in the world in recent years. Phase change materials (PCM), on the other hand, have an important property due to their thermal energy storage (TES) properties. Metal foams, porous medium or solid geometry, which are used in TES systems due to their important properties, are widely preferred to enhance the thermal performance of the PCM. The effects of porosity geometry, and porosity on the phase change material performance of porous domain have been investigated. Lattice structures or foams are used to create spaces in cellular structures [1]. During the recent years, porous domain ordered according to foam models due to its adjustable property, it creates a new potential heat transfer media. The additive manufacturing promotes the customization of these structures [2-3]. With this method, the production of parts in large geometric structures has become easier [4]. The use of heatsinks in electronic cooling systems has been studied in the studies of Qureshi et al. [5]. They found that the structure of triply periodic minimal surfaces (TPMS) fitted by additive manufacturing can reduce the temperature under high-temperature conditions for different pore geometries, heat fluxes, and PCMs. Fan et al. [6] aimed to enhance the efficiency of the battery by using paraffin wax combined with a battery thermal energy system (BTES) with TPMS of different geometric structures. With the system they used, they increased the efficiency of the battery by reducing the temperature increase. Three new porous TPMS heat sinks with computational fluid mechanics (CFD) have been modeled by Baobaid et al. [7]. TPMS-based heatsinks outperform conventional heatsinks in packing density and random distribution of flow. They found that porous

*Corresponding author: my.gokaslan@yyu.edu.tr

heatsinks are more promising. Catchpole-Smith et al. [8] and Qureshi et al. [9] obtained the same results in their numerical studies in TPMS, which they modeled, and in their experimental studies in PCM and embedded TPMS cages, respectively, and determine that the thermal conductivity of TPMS cages depends not only porosity but also on the structure of the TPMS cages. For increasing thermal performance, Hu et al. [10] designed a porous material as a heatsink, thermal conductivity enhancer and produced it with 3D printing. They shortened the operating time of the PCM by applying power to the systems they created with different porosity ratios with various heaters Hu et al. [10]. The development of 3D printing has led to its development, allowing porous media to be produced accurately and quickly [11,12]. Hasan and Tbena [13], studied a micro-channel heat sink (MCHS) with a PCM inside. They concluded that the cooling performance of PCMs was improved by using air first and then four different PCMs for cooling. Arshad et al. [14] carried out studies by examining the fins on electronic devices for the safer operation of electronic devices at low temperatures and prolonging their operating times. In other studies, Arshad et al. [15] stated that the use of PCM in cooling of electronic devices would be more efficient since phase change takes a long time. Gu et al. [16] studied the use of lattice structures showing that 2D lattice sandwich panels with continuous cross-section could be optimized for combined thermo-mechanical performance. The thermal performance and fabricated topology of PCM-optimized heat sinks were studied by Iradukunda et al [17]. As a result of their studies, they expressed that the heat sink they designed importantly increased PCM performance over a plate fin heat sink they selected as reference. The effect of porosity on periodic minimal surfaces (TPMS) with 3D printable geometrically complex structures was investigated by CFD modeling in the study of Hassan Ali et al. [18] convection coefficient, temperature and pressure drop values were estimated by CFD method using natural and forced convection effects in TPMS. Gopalan and Eswaran [19] used both PCM and porous structure to further increase conductivity in heat exchangers. In their results, they determined that the performance of the heat exchanger completely depends on the conductivity, and they found that the use of PCM together with the porous structure improves the conductivity.

The aim of the study is to increase energy savings and control the melting time thanks to a new multilayer hole network structures design using CFD. Then novelty of this study is that it is important in terms of its effects on the melt fraction and time of multilayer hole network structures with different surface geometries including PCM. Also, to show that this system can achieve some advantages without requiring additional energy.

2. PHYSICAL MODEL

The PCM was investigated by integrating it into the multi-layer structure as in Fig.1. Each layer is shown separately in Fig. 2. The geometric structure consists of three separate parts. There are cells of different diameter and number in each unit. The heat transfer performance of these cells of different diameters and their control over the PCM melt fraction are observed in terms of energy efficiency. Each layer has a 9 mm height and the height of the heater is 1 mm. The diameters of the holes and void volume in the structures are given in Table 1.

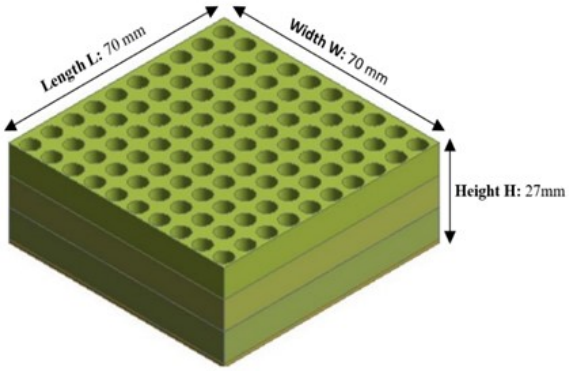

Figure 1. Multi-layer structure.

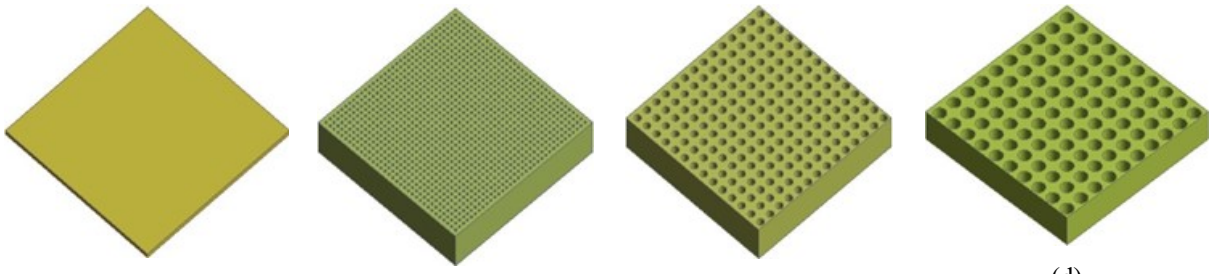

Figure 2. Parts of the physical model. (a) Heater, (b) Model 1, (c) Model 2, (d) Model 3.

Model 1 with a diameter of 5 mm, there are 10 cylindrical spaces on the horizontal axis, while there is solid geometry with a total length of 20 mm. In addition, there is solid geometry with a total length of 28 mm in Model 2 and 36 mm in Model 3. As the hole diameter increases, the void volume also increases. The void volume of the multilayer structures is 38311.7 mm^3.

Table 1 Cell diameters of physical model parts

Physical model	Cell diameter (mm)	Void volume (mm^3)
Model 1	5	17671.5
Model 2	3	12469.0
Model 3	1	8171.3

The initial and boundary conditions of this numerical study are below,

- The upper surface is fixed constant temperature which is 344 K,
- The side surfaces are fixed constant at isothermal boundary conditions,
- Constant heat flux is applied to base of the system which its value is 100 kW/m^2.
- The initial temperature is accepted 300 K.

Nazir et al. [20] studied the use of PCM, especially paraffin wax, in TES due to its advantages such as non-toxicity, latent heat of fusion and the fact that this heat does not deteriorate over time. The use of paraffin with metal foams to increase thermal performance which is melting time and melt fraction. The use of low-conductivity PCM in combination with a high-conductivity metal foam was explored by Rehman et al. [21]. The properties of PCM and metal used in the system were obtained by ref. [22], [23-25] and are summarized in Table 2. In this study, Organic paraffin was chosen as PCM. While selecting this organic paraffin, this choice was decided depending on the temperature required by the system. This selected PCM is defined as a new fluid in ANSYS.

Table 2 Thermophysical properties of the PCM and the material used in the study.

Material	Paraffin	AlSi10Mg
k (W/m^2)	0.2	175
ρ (kg/m^3)	880	2670
$\mathbf{c_p}$ (J/kgK)	2000	900
μ (kg/ms)	0.00365	-
β (1/K)	0.001	-
L (J/kg)	165000	-
$\mathbf{T_m}$ (K)	314	

3. GOVERNING EQUATIONS

The Boussinesq approach is used to model the melting of the PCM [26-27]. In addition, the continuity, momentum and conservation of energy equations for PCM are expressed as [28-29]:

Continuity equations

$$\nabla . u = 0 \tag{1}$$

Momentum equations

$$\rho_{PCM}\frac{\partial u}{\partial t} + \rho_{PCM}(u.\nabla)\mathrm{u} = -\nabla \mathrm{P} + \mu_{PCM}\nabla^2 u + \rho_{PCM} g\beta(T_{PCM} - T_m) - Au \tag{2}$$

where u, $\boldsymbol{\mu_{PCM}}$, $\boldsymbol{\rho_{PCM}}$ and $\mathrm{T_{PCM}}$ are the velocity, dynamic viscosity, density and temperature of the PCM. $\mathrm{T_m}$ is the PCM melting temperature, β is the volume expansion coefficient, g is the gravity acceleration, respectively. A is the source term by Eq. (3)

$$A = \frac{C_{mush}(1 - f_{PCM})^2}{\delta + f^3{}_{PCM}} \tag{3}$$

where f_{PCM} represent indicates the liquid fraction of PCM and it ranges from 0 to 1. 0 is the solid phase and 1 is the liquid phase, $\mathrm{C_{mush}}$ is the mushy zone parameter. It is defined as 10^5 based on ANSYS Fluent User's Guide [30].

Energy equations

$$\rho_{PCM} c_{p,PCM}\frac{\partial T_{PCM}}{\partial t} + \rho_{PCM} c_{p,PCM} u.\nabla T_{PCM} = \nabla.(k_{PCM}\nabla T_{PCM}) - \rho_{PCM} L\frac{\partial f_{PCM}}{\partial t} \tag{4}$$

where L, $\boldsymbol{k_{PCM}}$, $\boldsymbol{c_{p,PCM}}$ are the denotes the latent heat, thermal conductivity, specific heat capacity of the PCM, respectively. The $\boldsymbol{f_{PCM}}$ term is expressed in Eq. (5), depending on the temperature of the PCM:

$$f_{PCM} = \begin{cases} 0 & T_{PCM} \le T_{solid} \\ \dfrac{T_{PCM} - T_{solid}}{T_{liquid} - T_{solid}} & T_{solid} \le T_{PCM} \le T_{liquid} \\ 1 & T_{PCM} \ge T_{liquid} \end{cases} \tag{5}$$

where $\boldsymbol{T_{PCM}}$, T_{solid} and T_{liquid} are the PCM, the solid and liquid temperatures of the PCM, respectively. Heat transfer in metals (for aluminium) in Eq. (6):

$$\rho_s c_{p,s}\frac{\partial T_s}{\partial t} = \nabla.(k_s \nabla T_s) \tag{6}$$

where $\mathrm{T_s}$, $\mathrm{k_s}$, $\mathrm{c_{p,s}}$, and ρ_s, are thermophysical properties of solid which is aluminium. These terms represent temperature, thermal conductivity, specific heat capacity, and density, respectively.

Finally, the structure-PCM interface relation are given in Eq. (7) and Eq. (8)

$$T_f = T_s \tag{7}$$

$$k_f \frac{\partial T_f}{\partial n} = k_s \frac{\partial T_s}{\partial n} \tag{8}$$

4. NUMERICAL ANALYSIS

Commercial software ANSYS -Fluent was used to solve the governing equations. The finite volume method was used for the model's governing equations. In addition, for the thermophysical properties of paraffin and the solid are included in the model by writing a User Defined Function (UDF). The UDF used was obtained to be valid for the SI unit system. The SIMPLE algorithm was used for the solution of the equations. The residuals were set to 10^{-6}. The solutions were built using a 6-core processing unit. In addition, time step sensitivity analysis was taken into account in the analyses and was defined as 0.05 s for this analysis. Some assumptions made for PCM phase change to occur are given below:

• By ignoring the volume expansion of the PCM, the "Boussinesq" approach, which is embedded in the package program, is used in the density change of the fluid to perform the melting analysis.

• Flow; incompressible, laminar and Newtonian.

• The thermophysical properties of the metal and PCM are considered constant.

• The region where the PCM is neither liquid nor solid is considered mushy.

• Radiation and magnetic field are neglected.

Grid distribution

In this work, since the geometries obtained to determine the melting analyses in porous structures are not complex, network structures can be easily obtained. In Table 3, the properties of the meshes obtained for the layers of the physical model are given as nodes elements and average orthogonal quality values.

Table 3. Mesh parameters.

Physical model layers	Nodes	Elements	Average orthogonal quality
Model 1	988944	862564	0.94
Model 2	286566	237430	0.92
Model 3	150118	113554	0.96
Multi-layer structure	506557	414862	0.92

High orthogonal quality meshes were created. The average orthogonal quality values obtained by the appropriate meshing method show that those with results between 0.7-0.95 are in very good condition, and those with results between 0.95-1.00 are in excellent condition. As indicated in Table 4, the mesh structure converges after the certain value of the element size. The mesh sensitivity is applied for all cases.

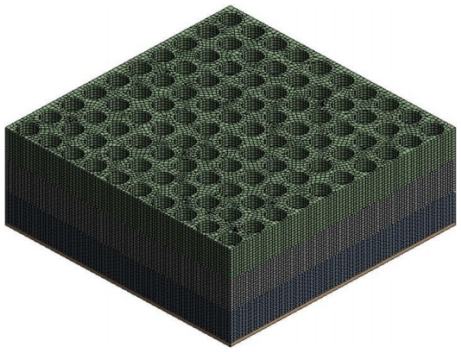

Figure 3. Mesh for the Multi-layer structure

The mesh sensitivity study was carried out to examine the variation of the converged solutions in each mesh with the solutions obtained using the mesh structures at different element size values of the same simulations. As it can be seen from the values in Table 4, the validity of the network structures formed as a result of the change in the absolute differences of the results obtained with this mesh sensitivity study at similar rates is proven. The element size value used for physical multi-layer structure is 70.

Table 4. Mesh sensitivity study for multi-layer structure.

Physical model	Element Size	Melt Fraction
Multi-layer structure	50	0.843
	55	0.847
	60	0.849
	65	0.853
	70	0.858

5. RESULT and DISCUSSION

In this section, the results obtained from the numerical simulations are explained and discussed. The results obtained separately for each layer were compared with the results of multi-layer structure obtained by combining all layers. The effects of the obtained results on the melting time are discussed. Melting curves and graphs for multi-layer structure are shown in Fig. 4-7. As seen in Fig. 4-5, the different axis states of the geometries, the transferred heat has positive effects on the melt fraction and the process by providing melting at the PCM and hole network structure interface.

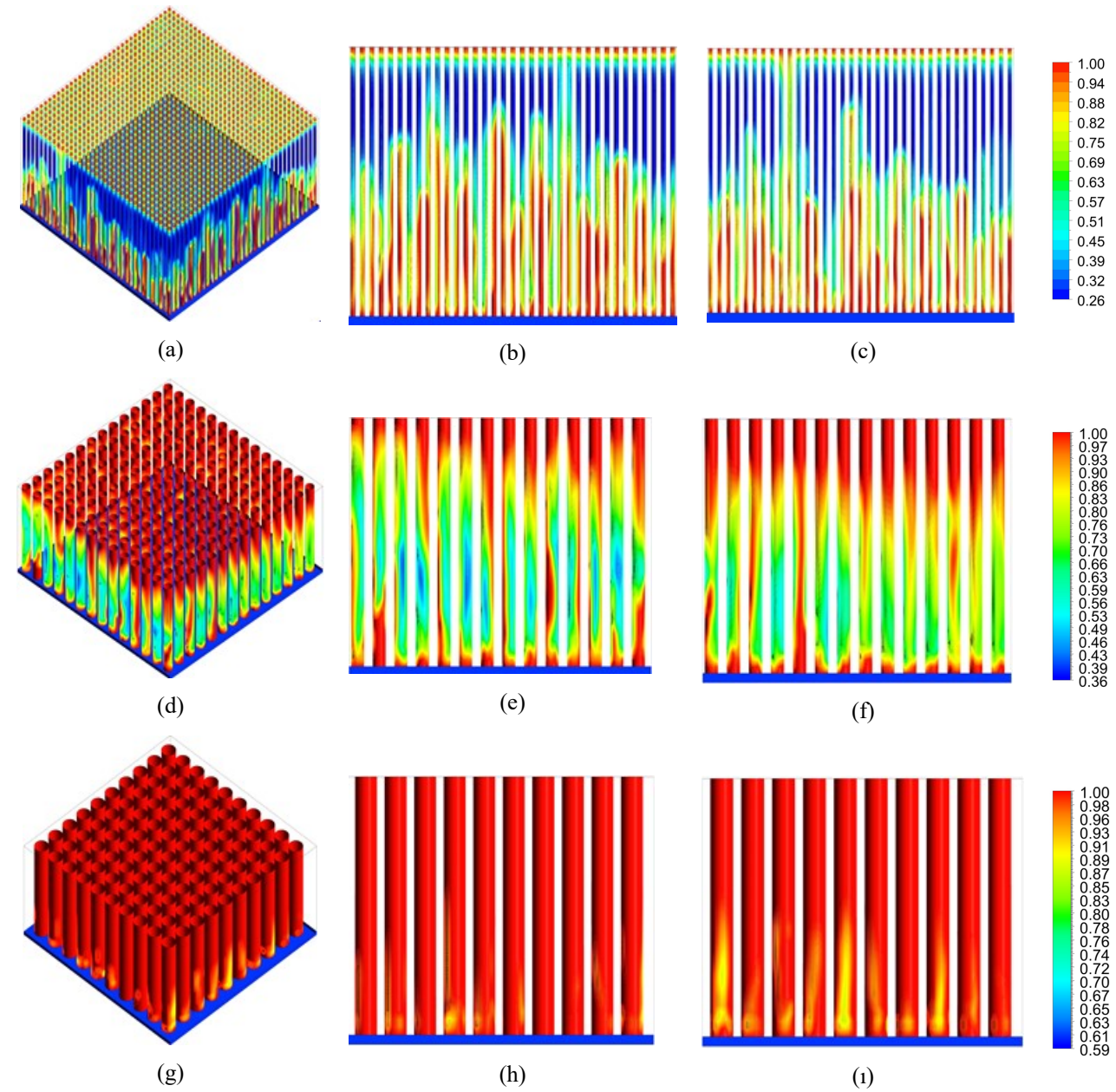

Figure 4. Liquid fraction of physical model layers at 500 s. (a) Model 1 view, (b) x-y axis view of Model 1, (c) y-z axis view of Model 1, (d) Model 2 view, (e) x-y axis view of Model 2, (f) y-z axis view of Model 2, (g) Model 3 view, (h) x-y axis view of Model 3, (ı) y-z axis view of Model 3.

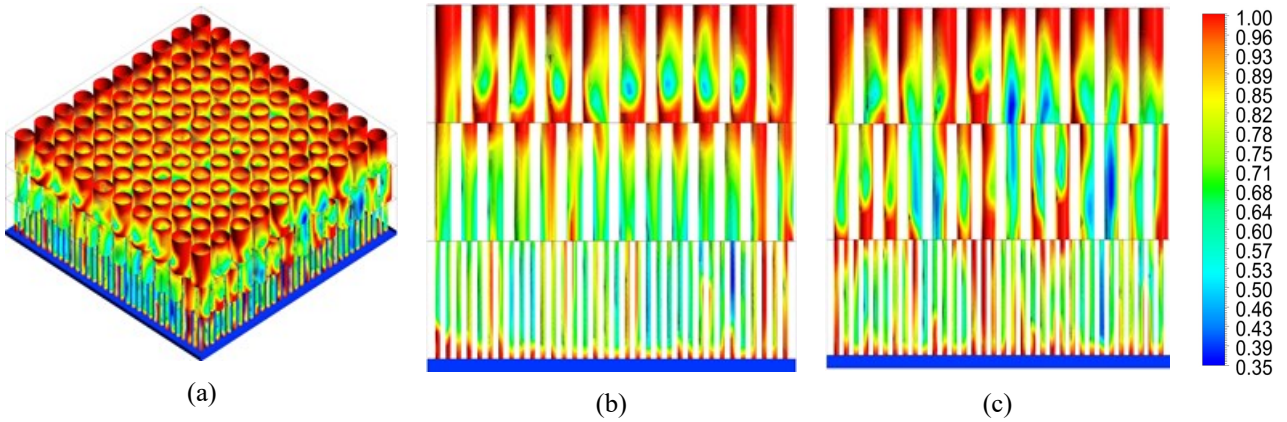

Figure 5. Liquid fraction of physical multi-layer structure at 500 s. (a) Multi-layer structure view, (b) x-y axis view, (c) y-z axis view

The presence of hole network structure for all cases improved melting. PCM properties are very important for melting time as most of the geometry volume is used by PCM. All melting graphs vary between 0-1. This means that the value of 0 is completely solid and the value of 1 is completely liquid.

The melting graphs of each layer at 500 s. are given in Fig. 4. Among the parameters affecting the melt fractions is the geometry of the structure, depending on the hole diameter. As shown in Fig. 6., when the layers of the physical model are examined separately, it is seen that the melt fraction in the Model 3 is closer to 1 than in the other physical models. This depends on the nature of the geometry in the Model 3. Under the same initial and boundary conditions, the melt fraction decreased as the hole diameter decreased. At the 300. s, the melt fraction of the geometry with the highest hole diameter is approximately 0.8, while the geometry with the lowest hole diameter is 0.6.

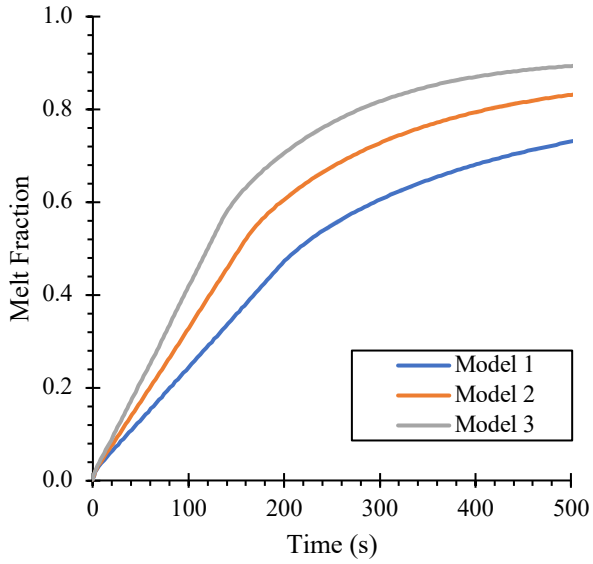

Figure 6. Melt fraction for different layers.

As can be seen in Fig. 5, the multi-layered hole network structure provided a proportionally more regular spread of the distribution of the melting contours over the geometry. It should be noted here that since each layer is placed on top of each other, the height is 27 mm and therefore the volume is equal to the sum of these three geometry volumes. The void volume is the geometry with the highest value.

Figure 7 shows relation the melt fraction of the multilayer structure between time. Also, the melt fractions of each layer are also given for comparison. The melt fraction of the multilayer structure shows closer to the Model 2 and between the melting fractions of the Model 3 and Model 2 structure. However, the void volume of the Model 2 is 12469 mm^3, while the void volume of the multi-layer structure is 38311.7 mm^3. It is determined that the phase change material with approximately three times higher volume provides better thermal performance under the same initial and boundary conditions. As indicated in the graph in Fig. 7., At 500 s., the melt fractions are between 0.8-0.9 for multi-layer structure, between 0.9-1.0 for the Model 3, between 0.8-0.9 for the Model 2, and between 0.8-0.9 for the Model 1.

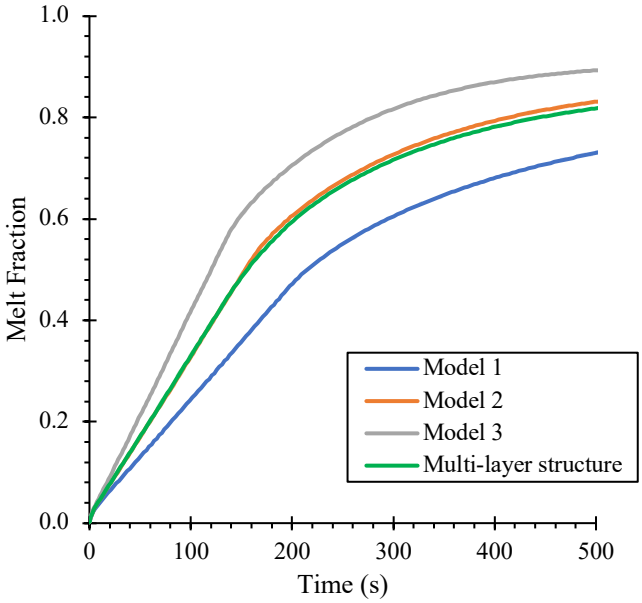

Figure 7. Comparison of melt fraction.

It is expected that the multi-layered structure may have a positive effect on the melting performance. However, although the analyzes are performed under the same conditions, the void volumes of each layer and multi-layer structures are not the same. The multi-layer structures exhibited better thermal performance despite having five times the void volume than the Model 1. When multi-layer structure and the Model 3 structure are compared, it is seen that the thermal performance of the Model 3 structure is better. However, the structure on the Model 3 has almost half the void volume compared to the other. This is the most important factor affecting the melt fraction and time.

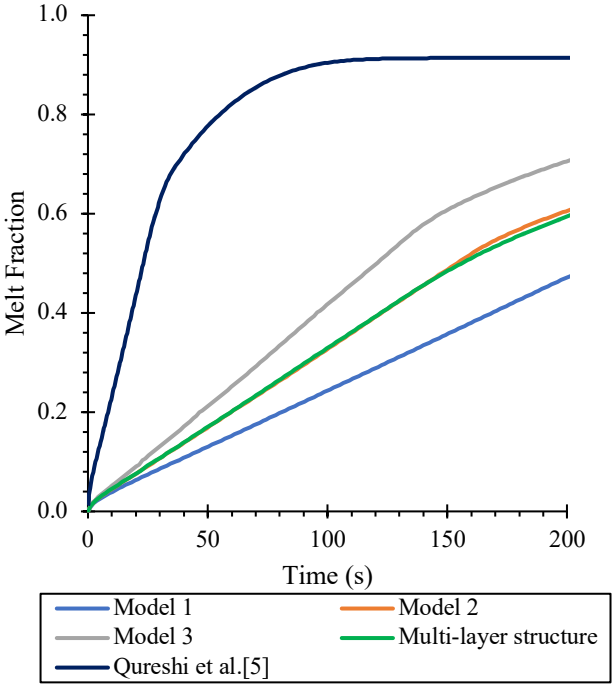

Figure 8. Validation of the study with literature.

Qureshi et al. [5, 28] carried out melting analysis using dimensions and materials with similar properties in their numerical studies. The validity of this study, Qureshi et al. [5] was chosen for comparison. The melting data obtained as indicated as seen in in Fig. 8. Using the same heat flux in their work, Qureshi et al. [5] determined that the melt fraction was approximately 0.9 in the Kelvin model at 200 s. Aluminum was used as solid material and docosane which is an organic PCM was used as phase change material in their study. In this study, the melting rate in the 200 s. multi-layer model is approximately 0.6. Compared to this study, the Authors's [5] work had a melting rate of 0.9 in 100 s., while the melt fraction in the multi-layer is about 0.35 at this time. This difference in comparison also depends on the mass of the phase change material in the models. In this numerical study, the melting time is longer and the melt fraction curve is linear. This may provide an advantage according to the usage area of these models.

6. CONCLUSION

The effects of PCM melt fraction and melting time on the hole network structures design obtained by combining multilayer hole network structures with different diameters were investigated. Thus, 3D analyses were conducted for each layer separately and for the geometry obtained by combining all layers. Initial and boundary conditions are equal for all cases. The results show that the melting time of the multilayer structure showed approximately close results with other layered structures. However, the melting formed in the multi-layered structure reveals a more regular distribution compared to other structures, in this case, it states that the study can provide an advantage for melting. The melting time and rate of the multi-layer structure are very similar to the Model 2 structure, but the distribution of the melting contours is more even and regular in all regions.

In the analyses performed for the PCM selected in the study and the initial temperature, the melt fractions vary between 0.8-0.9 values. This situation shows that %80 melting occurred in the analysed geometries. Studies can be improved to increase the melt fraction. In future studies, the melting temperature of the selected PCM can be selected differently or the initial temperature can be changed in order to obtain analyses where the melt fraction is 1 and 100% melting is achieved. There are two recommendations for the geometries in this study, either the PCM used should be replaced with a PCM with a lower melting temperature or the initial temperature should be increased without changing the PCM. Thus, the melt fraction will be improved for the work done.

The void volumes of the analysed geometries are different from each other as shown in Table1. The melting performance is better in the multi-layer structure with the void volume higher in the Model 1 and Model 2. However, the melt fraction of the multilayer structure is worse than the Model 3. The reason for this is that the void volume of the multi-layer structure is higher, and therefore the phase change material is more. In order to see the thermal performance difference between these two geometries more clearly, the analyses should be repeated when the void volumes are the same.

As a future study, heat flux power, solid material, PCM material, geometry dimensions and layer locations can be modified to better understand the thermal performance and effects of parameters which is effects of design variables. In addition, in order to better comparison of results, the geometric heights of each model can be adjusted so that the void volume is the same and they can be compared.

REFERENCES

[1] Mazur, M., Leary, M., McMillan, M., Sun, S., Shidid, D., Brandt, M. 2016. Mechanical properties of Ti6Al4 and AlSi12Mg lattice structures manufactured by Selective Laser Melting (SLM), *Elsevier Science & Technology*, 1 (5):119-161.

[2] Yang, L., Harrysson, O., Cormier, D., West, H., Gong, H., Stucker, B. 2015. Additive manufacturing of metal cellular structures: Design and Fabrication, *The Minerals, Metals & Materials Society*, 3 (67):608-615.

[3] Thompson, M., K., Moroni, G., Vaneker, T., Fadel, G., Ian Campbell, R., Ian, G., Bernard, A., Scuhulz, J., Graf, P., Ahuja, B., Martina, F. 2016. Design for additive manufacturing: Trends, opportunities, considerations and constraints*, CIRP Annals*, 2 (65):737-760.

[4] Al-Ketan, O., Rowshan, R., Al-Rub, R., K., A. 2018. Topology-mechanical property relationship of 3D printed strut, skeletal and sheet based periodic metallic cellular materials, *Additive Manufacturing*, 19:167-183.

[5] Qureshi, Z., A., Elnajjar, E., Al-Ketan, O., Al-Rub, R., A., Al-Omari, S., B. 2021. Heat transfer performance of a finned metal foam-phase change material (FMF-PCM) system incorporating triply periodic minimal surfaces (TPMS), *International Journal of Heat and Mass Transfer*, 170:121-001.

[6] Fan, Z., Fu, Y., Gao, R., Liu, S. 2023. Investigation on heat transfer enhancement of phase change material for battery thermal energy storage system based on composite triply periodic minimal surface, *Journal of Energy Storage*, 57 (14):106-222.

[7] Baobaid, N., Ali, M., I., Khan, K., A., Al-Rub, R., K., A.. 2022. Fluid flow and heat transfer of porous TPMS architected heat sinks in free convection environment, *Case Studied in Thermal Engineering*, 33:101-944.

[8] Catchpole-Smith, S., Sélo, R., R., J., Davis, A., W., Ashcroft, I., A., Tuck, C., J., Clare, A. 2019. Thermal conductivity of TPMS lattice structures manufactured via laser powder bed fusion, *Additive Manufacturing*, 30:100-846.

[9] Qureshi, Z., A., Al Omari, S., A., B., Elnajjar, E., Mahmoud, F., Al-Ketan, O., Al-Rub, R., A. 2021. Thermal characterization of 3D-Printed lattices based on triply periodic minimal surfaces embedded with organic phase change material, *Case Studies in Thermal Engineering*, 27 (3):101-315.

[10] Hu, X., Gong, X. 2021. Experimental study on the thermal response of PCM- based heat sink using structured porous material fabricated by 3D printing*, Case Studies in Thermal Engineering*, 24:100-844.

[11] Ngo, T., D., Kashani, A., Imbalzono, G., Nguyen, K., T., Q., Huis, D. 2018. Additive manufacturing (3D printing): A review of materials, methods, applications and challenges, *Composites Part B Engineering*, 143:172-196.

[12] Maiti, A., Small, W., Lewicki, J., P., Weisgraber, T., H., Duoss, E., B., Chinn, S., C., Pearson, M., A., Spadaccini, C., M., Maxwell, R., S., Wilson, T., S. 2016. 3D printed cellular solid outperforms traditional stochastic foam in long-term mechanical response, *Scientific Reports*, 25 (6):24871.

[13] Hasan, M., I., Tbena, H., L. 2018. Using of phase change materials to enhance the thermal performance of micro channel heat sink, *Engineering Science and Technology an International Journal*, 3 (21):517-526.

[14] Arshad, A., Ali, H., M., Ali, M., Manzoor, S. 2017. Thermal performance of phase change material (PCM) based pin-finned heat sinks for electronics devices: Effect of pin thickness and PCM volume fraction, *Applied Thermal Engineering*, 112:143-155.

[15] Arshad, A., Ali, H., M., Khushnood, S., Jabbal, M. 2018. Experimental investigation of PCM based round pin-fin heat sinks for thermal management of electronics: Effect of pin-fin diameter*, International Journal of Heat and Mass Transfer*, 117:861-872.

[16] Gu, S., Lu, T., J., Evans, A., G. 2001. On the design of two-dimensional cellular metals for combined heat dissipation and structural load capacity, *International Journal of Heat and Mass Transfer*, 11 (44):2163-2175.

[17] Irandukunda, A., C., Vargas, A., Huiting, D., Lohan, D. 2020. Transient thermal performance using phase change material integrated topology optimized heat sink, *Applied Thermal Engineering*, 2 (179):115-723.

[18] Ali, M., I., H., Al-Keetan, O., Khalil, M., Baobaid, N. 2020. 3D printed architected heat sinks cooling performance in free and forced convection environments, Proceedings of the ASME 2020 Heat Transfer Summer Conference, HT2020-9067.

[19] Gopalan, K., S., Eswaran, V. 2016. Numerical investigation of the thermal performance of PCM based heat sink using structured porous media as thermal conductivity enhancers, *International Journal of Thermal Sciences*, 104:266-280.

[20] Nazir, H., Batool, M., Osorio, F., J., B., Isaza-Ruiz, M., Xu, X., Vignarooban, K., Phela, P., Inamuddin, Kannan, A., M. 2019. Recent developments in phase change materials for energy storage applications: A review, *International Journal of Heat and Mass Transfer*, 129:491-523.

[21] ur-Rehman, T., Ali, H., M., Janjua, M., M., Sajjad, U., Yan, W-M. 2019. A critical review on heat transfer augmentation of phase change materials embedded with porous materials/foams, *International Journal of Heat and Mass Transfer*, 135:649-673.

[22] RT-42, data sheet https://www.rubitherm.eu/media/products/datasheets/Techdata_-RT42_EN_09102020.PDF (Accessed on July 12, 2023)

[23] Zhang, Z., He, X. 2016. Three-dimensional numerical study on solid-liquid phase change within open-celled aluminium foam with porosity gradient, *Applied Thermal Engineering*, 113:9-10.

[24] Zhu, F., Zhang, C., Gong X. 2017. Numerical analysis on the energy storage efficiency of phase change material embedded in finned metal foam with graded porosity, *Applied Thermal Engineering*, 123:256–265.

[25] AlSi10Mg, data sheet https://software.xactmetal.com/md/datasheets/Material%20Data%20Sheet%20-%20AlSi10Mg.pdf (Accessed on July 12, 2023)

[26] Brent, A., D., Voller, V., R., Reid, K., J. 2007. Enthalpy-porosity technique for modelling convection-diffusion phase change: Application to the melting of a pure metal, *Numerical Heat Transfer*, 3 (13):297–318.

[27] Mahdi, M., Khadom, A., A., Mahood, H., B., Yaqup, M., A., R., Hussain, J., M., Salih, K., I., Kazem, H., A. 2019. Effect of fin geometry on natural convection heat transfer in electrical distribution transformer: Numerical study and experimental validation, *Thermal Science and Engineering Progress*, 4 (14):100–414.

[28] Qureshi, Z., A., Al-Omari, S., A., B., Elnajjar, E., Al-Ketan, O., Al-Rub, R., A. 2022. Architected lattices embedded with phase change materials for thermal management of high-power electronics: A numerical study, *Applied Thermal Engineering*, 22:01350–3.

[29] Moon, C., Kim, H., D., Kim, K., C. 2018. Kelvin-cell-based metal foam heat exchanger with elliptical struts for low energy consumption, *Applied Thermal Engineering*, 144:540-550.

[30] ANSYS 18 Fluent User's Guide 2018